Semi-Discrete Scheme for the Solution of Flow in River Tinnelva

Susantha Dissanayake Roshan Sharma Bernt Lie

Department of Electrical Engineering, IT, and Cybernetics, University College of Southeast Norway, Porsgrunn, Norway, {roshan.sharma, bernt.lie}@usn.no

Abstract

The Saint-Venant equation is a mathematical model which could be used to study water flow in an open channel, river, etc. The Kurganov-Petrova (KP) method, which is a second-order scheme, is used to solve the Saint-Venant equations with good stability. The water flow of a river between two hydropower stations in Norway has been simulated in this study using MATLAB and OpenModelica. The KP scheme has been used to discretize the Saint-Venant equations in the spatial domain, yielding a collection of Ordinary Differential Equations (ODEs). These are then integrated with time using the variable step-length solvers in MATLAB: ode23t, ode23s, ode45, and fixed step-length solvers: The Euler method, the second and fourth order Runge Kutta method (RK2 and RK4). In OpenModelica built-in, variable step-length DASSL solver has been used. From the simulation, it was observed that all solvers produce more or less similar results. Volumetric flowrate calculation indicated numerical oscillation with variable step-length solvers in MATLAB. The results indicated that it is reasonable to match the order of space and time discretization.

Keywords: semi-discrete KP scheme, OpenModelica, MATLAB

1 Introduction

By the year 2020, the 20-20-20 goal is to be achieved within the European Union: 20% efficiency in the improvement of power utilization, 20% reduction of carbon dioxide emission and 20% increment of renewable sources in the total energy mix (Blindheim, 2015). Subsequently, the utilization of renewable energy sources such as wind, hydro, and solar have to be optimized. Hydropower is a source of kinetic energy, which is extracted from flowing water. It is one of the mature renewable energy technologies in the current energy sector.

Norway is prominent in the production of hydropower as one of the renewable energy sources (Blindheim, 2015). Even though reservoir based power production technologies are well developed, power generation based on run-of-river systems are also common. As several hydropower stations are installed at different locations along the same river length, water flow between different hydropower stations influence their operations. When the upstream station (first station) increases its power production, volumetric flow of water out from the first station increases, thus the downstream power station (second station) has to increase the power production in order to utilize the water resource efficiently (Vytvytskyi et al., 2015).

Hence, it is vital to have an understanding of the propagation of the water flow from one station to the other, the change of water level at the second dam, the speed of the wave that hits the second dam, etc. Water flow modeling is also useful in other areas, e.g., managing water resources efficiently in agriculture, manage municipal drinking water distribution system and other applications in addition to power generation.

In this study, the flow of water in river Tinnelva in Southeast Norway between two hydropower stations are being considered. One power station is located at Årlifoss, and the other station is located at Grønvollfoss (downstream). The aim is to study the use of a semi-discrete scheme for the solution of flow in river Tinnelva. Objectives are to find an accurate and robust scheme for use in the control algorithm.

The paper is arranged as follows. The basic introduction to the governing equation and computational fluid dynamics (CFD) will be given in Section 2. Introduction to the KP numerical scheme will be provided in Section 3. Section 4 focuses on computer simulation. The Saint-Venant equation and the Kurganov-Petrova (KP) scheme as numerical scheme were used in simulation in order to compute final water level at Grønvollfoss dam. MATLAB and OpenModelica are being used as simulation software, and both built-in, variable step-length solvers and fixed step-length solvers are being used for the time integration. Parameters, assumptions, simplifications of the complex river system are also introduced in Section 4. Simulation results will be discussed in Section 5 together with numerical stability analysis.

2 Governing Equation for Flow Modeling

Conservation of properties of fluid flow, such as mass, energy, and momentum equations are important principles in fluid dynamics (Versteeg and Malalasekera, 2007). For the study of wave propagation, water flow, tsunami, etc. mathematical models have been derived based on the continuity equation and the momentum balance (Fayssal et al., 2015).

The Saint-Venant equation or commonly known as the 1-Dimensional (1D) shallow water equation, is used for decades for simulation of water flow in open channels, rivers, etc. (Benkhaldoun et al., 2015). Basic conservation laws, such as momentum and mass conservation provide the base for the Saint-Venant equation which has been derived by integrating the momentum equation over the vertical coordinate (Benkhaldoun et al., 2015). This model provides stable solutions even at hydraulic jumps. The Saint-Venant equation can be posed as follows (Sharma, 2015).

$$\frac{\partial U}{\partial t} + \frac{\partial F}{\partial x} = S \tag{1}$$

where U vector is the vector of conserved variables

$$U = (A, Q)^T \tag{2}$$

F is the vector of fluxes

$$F = \left(Q, \frac{Q^2}{A} + gI_1 \cos(\phi)\right)^T \tag{3}$$

and S is the source term

$$U = (z, q)^T, \tag{4}$$

$$F = \left(q, \frac{q^2}{z-B} + \frac{g}{2}(z-B)^2\right)^T, \tag{5}$$

$$S = \left(0, -g(z-B)\frac{\partial B}{\partial x} + \frac{gn^2 q|q|\left(w+2(z-B)\right)^{\frac{4}{3}}}{w^{\frac{4}{3}}} \frac{1}{(z-B)^{\frac{7}{3}}}\right). \tag{6}$$

Here, z is the water level above a datum, B is the bottom elevation from the datum, q is volumetric flow rate per unit width, w is the width of the river, n is Mannings roughness coefficient, and g is acceleration due to gravity. The S terms reflect source terms: including expressions of friction which give resistance against flow.

3 KP Numerical Scheme

In computational Fluid Dynamics (CFD), The Finite Volume Method (FVM) is based on averaging the Control Volume (CV) (Kurganov and Tadmor, 2000). As FVM average each CVs, discontinuities may occur at CV interfaces. This problem was recognized as the Riemann problem (Kurganov and Levy, 2002). In order to handle the Riemann problem, the Riemann solvers were developed (Kurganov and Tadmor, 2000). However, by the emerging of computer-based complex calculations, fast convergence with higher accuracy has to be accomplished. Subsequently, several novel techniques that could eliminate Riemann solvers were developed. The KP scheme was one of the developments which could handle discontinuities at CV interfaces without the Riemann solvers (Kurganov and Tadmor, 2000). The KP scheme is semi-discrete in nature: discretization in space and Ordinary Differential Equation (ODE) solvers in MATLAB and OpenModelica can be used to solve the resulting differential algebraic equations.

Kurganov and Petrova have developed a new scheme which could be considered as an extension/further development of the Nessyahu-Tadmor (NT) scheme (Kurganov and Tadmor, 2000). The NT scheme was developed to average the CV value by using the non-smooth Riemann fans over a fixed length $\triangle x$ (Nessyahu and Tadmor, 1990). In the KP scheme development, instead of averaging the non-smooth parts of the Riemann fans, precise local velocities of wave propagation have been considered along with small CVs of variable size (Kurganov and Tadmor, 2000). When the CV interface has discontinuities, a staggered CV concept can be introduced to eliminate the problem (LeVeque, 1999). During the transient, the local velocities are usually different at each side of a CV interface. Therefore, altered staggering at both sides of the CV is reasonable. Thus, the size of the virtual CVs are defined for a small time ($\triangle t$) by considering the local velocity of wave propagation. For each non-uniform CVs, a piecewise linear reconstruction has been done over the solution domain. Later the linear reconstructed values have been projected to the original uniform CVs while assuming the limits $\triangle t \to 0$ (Kurganov and Tadmor, 2000).

In the KP scheme, properties are indexed by a plus (+) and minus (-) with reference to the direction of the property flux. The local speed of discontinuity propagation has been calculated by considering the Jacobi matrix of the governing equations. In order to achieve higher resolution and a well-balanced scheme, the Total Variant Diminishing (TVD) concept together with the flux limiter concept has been used. The standard *minmod* limiter has been used in the original development of the KP scheme; many alternative flux limiters can be used just as well (Kurganov and Tadmor, 2000).

The KP scheme does not use the Riemann solvers. Hence, computational time can be reduced. Numerical viscosity with the KP scheme is lower compared to the NT scheme (Kurganov and Tadmor, 2000).

The KP scheme discretizes the Saint-Venant equation spatially, yielding a collection of ODEs in time. These ODEs can be written as follows,

$$\frac{d}{dt}\bar{u}_j = -\frac{H_{j+\frac{1}{2}}(t) - H_{j-\frac{1}{2}}(t)}{\triangle x}, \tag{7}$$

where $\bar{u}_j$ is the cell center average values, $H_{j\pm\frac{1}{2}}(t)$ are the central upwind numerical fluxes at the cell interfaces, defined as:

$$H_{j+\frac{1}{2}}(t) = \frac{a^+_{j+\frac{1}{2}} F\left(u^-_{j+\frac{1}{2}}, B_{j+\frac{1}{2}}\right) - a^-_{j+\frac{1}{2}} F\left(u^+_{j+\frac{1}{2}}, B_{j+\frac{1}{2}}\right)}{a^+_{j+\frac{1}{2}} - a^-_{j+\frac{1}{2}}} + \frac{a^+_{j+\frac{1}{2}} a^-_{j+\frac{1}{2}}}{a^+_{j+\frac{1}{2}} - a^-_{j+\frac{1}{2}}}\left(u^+_{j+\frac{1}{2}} - u^-_{j+\frac{1}{2}}\right), \tag{8}$$

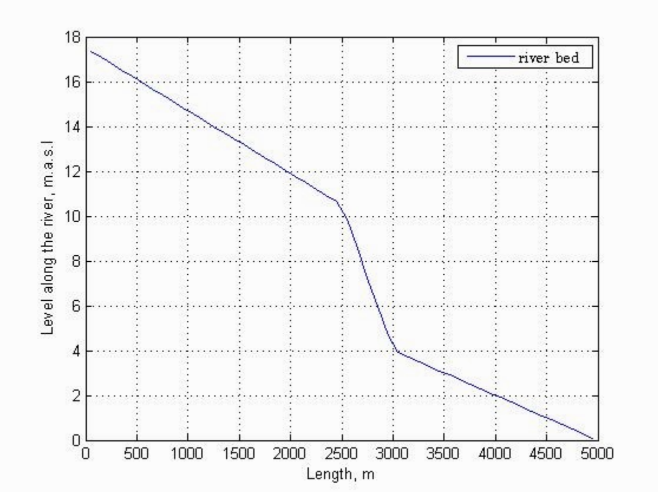

Figure 1. Bottom topography of the river.

$$H_{j-\frac{1}{2}}(t) = \frac{a^+_{j-\frac{1}{2}} F\left(u^-_{j-\frac{1}{2}}, B_{j-\frac{1}{2}}\right) - a^-_{j-\frac{1}{2}} F\left(u^+_{j-\frac{1}{2}}, B_{j-\frac{1}{2}}\right)}{a^+_{j-\frac{1}{2}} - a^-_{j-\frac{1}{2}}} + \frac{a^+_{j-\frac{1}{2}} a^-_{j-\frac{1}{2}}}{a^+_{j-\frac{1}{2}} - a^-_{j-\frac{1}{2}}} \left(u^+_{j-\frac{1}{2}} - u^-_{j-\frac{1}{2}}\right), \quad (9)$$

where $a^{\pm}_{j\pm\frac{1}{2}}$ are the one-sided local speeds of propagation and $u^{\pm}_{j\pm\frac{1}{2}}$ are property fluxes at indexed positions (Sharma 2015).

4 Simulation of the River Flow

In river Tinnelva, two hydropower stations, one at Årlifoss, and the other at Grønvollfoss are being operated by Skagerak Energi. The river reach is 5km in length. In the study, the bottom topography of the river has been divided into three sections of different slope, and the width of the river is assumed to be constant (180 m) during the whole reach of interest. The assumed bottom topography of the river is illustrated in Figure 1. The section from 2.5 km to 3 km has a steeper bed compared to the other sections (Vytvytskyi et al., 2015).

Due to different operational conditions, the volumetric outflow of water at the Årlifoss station is varying. The volumetric flow rates and other quantities are displayed in Table 1.

Other than the spatial discretization done by the KP scheme, time discretization methods in fixed step-length: The Euler method, the second order, and the fourth order Runge Kutta (RK2 and RK4) and the built-in variable step-length solvers: ode solvers in MATLAB (ode23s, ode23t, ode45) and the DASSL solver in OpenModelica, have been used. In addition to the water level computation, the numerical stability of each solver has been analyzed. Here, only for the numerical stability analysis, the variable step-length ode15s solver has been used.

Table 1. Results analysis.

Length	5 km
Number of CV	200
Time steps ($\triangle t$)	0.25 s
Volumetric flow in	120 m^3/s
Volumetric flow out	120 m^3/s
Volumetric flow increased	160 m^3/s
Width of the river	180 m
Initial water level at the dam	17.5 m
Mannings friction factor	0.04 $s/m^{1/3}$
Gravitational constant	9.81 m/s^2

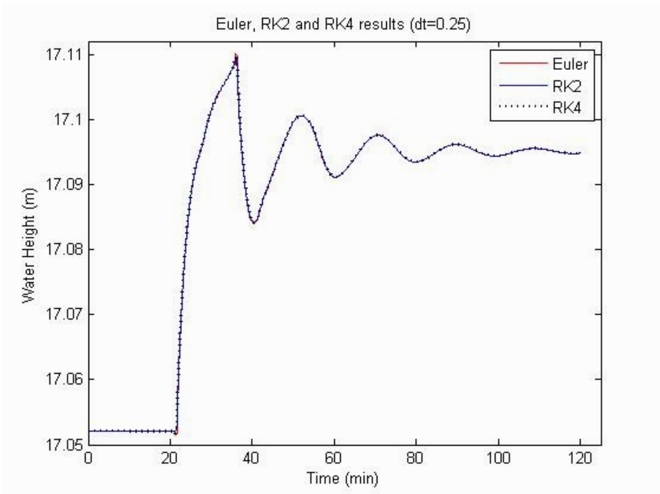

Figure 2. Fixed step-length solvers the Euler method, RK2, RK4 ($\triangle t = 0.25s$).

5 Results and Discussion

Results of the simulation study and numerical stability analysis will be discussed in the following sub sections.

5.1 Simulation Results

The built-in variable step-length solvers: ode23t and ode23s have second-order accuracy (Gladwell et al., 2003). Fixed step-length solvers: The Euler method, the RK2 method, and the RK4 method have first order, second order, and fourth order accuracy respectively (Gerald and Wheatley, 2004; LeVeque, 1992). ode45 and ode15s have higher order; higher than a second order of accuracy (Gladwell et al., 2003).

The simulation results using fixed step-length solvers (the Euler method, the RK2 method and the RK4 method) with fixed step length ($\triangle t$ = 0.25 second) show very similar behaviors as shown in Figure 2.

An exploded view of Figure 2 in the time range of 35 min to 37 min is shown in Figure 3. In the exploded view, the Euler method shows some deviation from the other two solutions. However, this deviation is very small.

Both RK2, RK4 and the Euler method algorithms show accuracy up to fourth significant digits in their final solu-

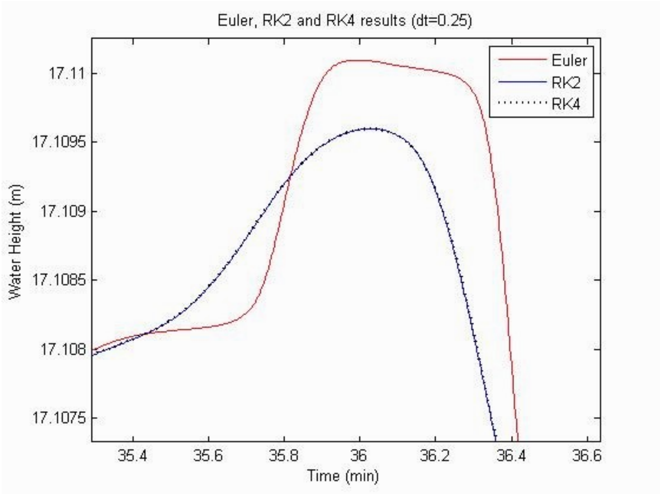

Figure 3. Exploded view of fixed step-length solvers (Euler method, RK2, RK4).

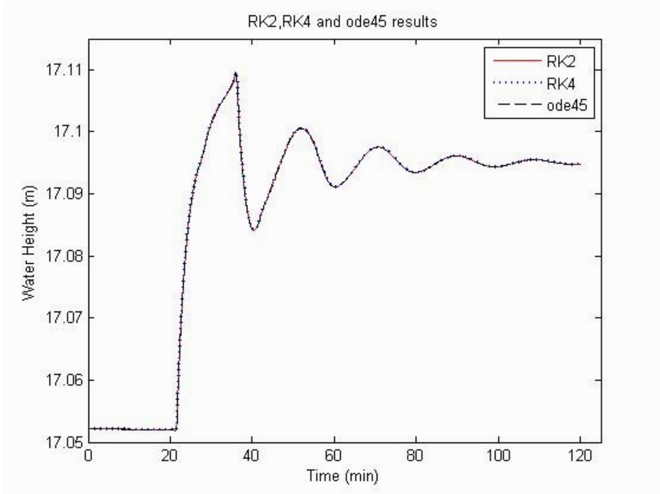

Figure 5. The RK2, RK4 method and ode45 solver results at $\triangle t$ = 0.25 s.

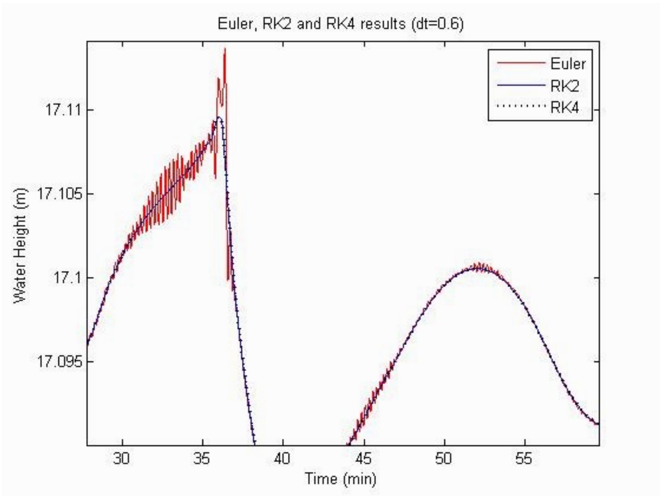

Figure 4. Fixed step-length solvers the Euler method, RK2, RK4 at $\triangle t$ = 0.6 s.

tions.

The solution obtained using the Euler method is highly dependent the choice of the step length; $\triangle t$. When $\triangle t$ is set to 0.6 seconds, the Euler method shows some oscillation in its solution (Figure 4).

With $\triangle t$ set to 0.7 seconds, the solution becomes unstable. While The Euler method shows higher oscillatoric behavior and unstable solutions when $\triangle t$ increases ($\triangle t \geq$ 0.7s) the RK2 and RK4 methods produce stable solutions. However, increment of $\triangle t$ has necessarily to be agreed with the CFL condition (Silvester et al., 2015; LeVeque, 1992) which is commonly written as,

$$C = \frac{u\triangle t}{\triangle x} \leq C_{max} \tag{10}$$

Here C is dimensionless number u refers the magnitude of the velocity, $\triangle x$ refers the length of CV. For the upwind scheme, $C_{max} = 1$ (Silvester et al., 2015).

The standard KP scheme is a second order scheme in spatial discretization (Kurganov and Tadmor, 2000). Higher order time integrators: the RK4 method and ode45 were used to solve second order ODEs returned by spatial discretization of the Saint-Venant equation.

The idea was to check whether the higher order time integrators; higher than the second order, have a significant influence on solving second order ODEs more accurately.

According to the observations, both RK2 and the RK4 schemes show very similar solutions. Hence, this denotes that the higher order time integrators have the minor influence on the accuracy when it uses to solve lower order ODEs. The selection of an order of the time discretization that exceeds the order of the spatial discretization does not necessarily produce a more accurate solution (Liu and Tadmor, 1998). Consequently, in order to acquire a reasonably accurate solution, the order of the time discretization should be of either lower or the same order as the order of the spatial discretization.

When comparing variable step-length ode45 solvers in MATLAB with fixed step-length solvers: RK2 and RK4, all solvers produce very similar results (Figure 5). In exploded view (Figure 6), the variable step-length solver ode45 shows some minor oscillatory behavior. Even though the exploded view shows a small deviation, the results of the all three solvers (ode45, RK2, and RK4) compute the end-time water height at the Grønvollfoss dam accurately up to the fourth significant digit.

Results of all fixed step-length solvers: The Euler method, RK2, RK4 and all variable step-length solvers: ode23s, ode23t, ode45 are shown in Figure 7. The computed final water height of each different solver are similar (Figure 7), however, when it considers closely zooming in, it is possible to see minor deviations.

OpenModelica simulation by using the built-in DASSL solver shows a similar pattern compared to the solutions of the MATLAB solvers as shown in Figure 8. Table 2 sum-

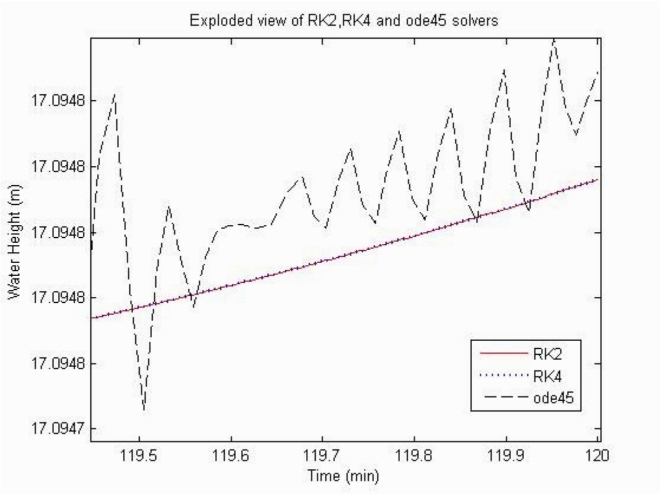

Figure 6. Exploded view of the RK2, RK4 method and ode45 solver results at $\triangle t$ = 0.25 s.

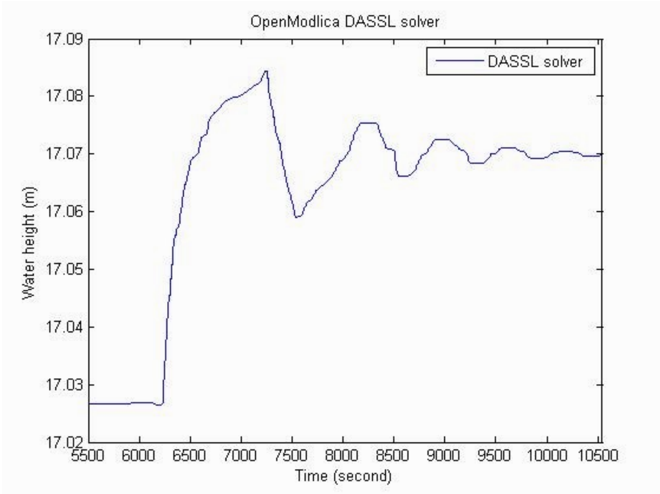

Figure 8. OpenModelica simulation results with DASSL solver.

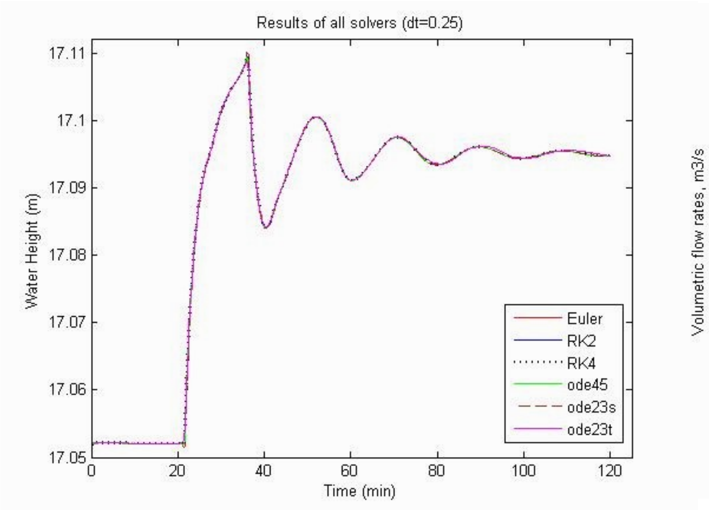

Figure 7. All solvers result at $\triangle t$ = 0.25 s.

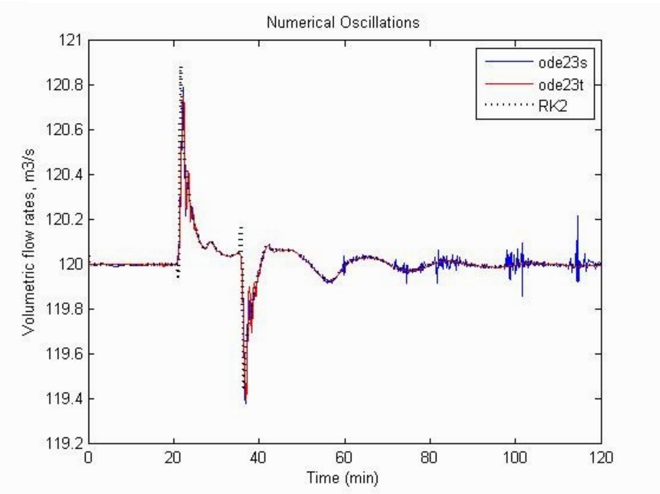

Figure 9. Numerical oscillation of group 01 solvers $\triangle t$ = 0.25 s.

marizes other observations of the simulation study. Time consumed by each solver, minimum and maximum time step of variable step-length solvers and steady water level for all solvers are tabulated in the Table 2.

5.2 Simulation Results for Numerical Stability Analysis

In this section, results of numerical stability analysis will be discussed. For ease of comparison, the six solvers, which were used, have been divided into two groups based on their order of the accuracy. Thus, ode23s, ode23t and the RK2 method were classed into group 01, which are of second order in accuracy. The RK4, ode45 and ode15s solvers were classed into the group 02, which are of higher order in accuracy in time discretization than group 01.

The results of the volumetric flow rate calculation for the lower order group (group 01) are plotted in Figure 9. From the observations, the ode23s and ode23t solvers show higher oscillation in volumetric flow rate calculations than RK2.

For the results of the group 02 solvers, Figure 10, it can be clearly seen, that the oscillatory nature increases with increasing order of the time discretization. The solution using variable step-length ode solvers are more oscillatory compared to the fixed step-length solvers RK4 for the volumetric flowrate calculations. ode45 shows higher oscillation while ode15s show relatively smaller oscillations for the volumetric flow rate calculation.

As a whole, it could be observed that built-in variable step-length ode solvers show a relatively oscillatory nature for the volumetric flow rate calculations.

6 Conclusions

Based on the simulated results, it can be concluded that a higher order in the time discretization than the order in the spatial discretization does not necessarily produce more accurate solutions, consequently, matching orders of both

Table 2. Results analysis.

Description	*Solver*	*Values*
Computational time at $\triangle t$ = 0.25 in seconds	ode23t (variable step-length)	11
	ode23s (variable step-length)	325
	ode45 (variable step-length)	15
	ode15s (variable step-length)	125
	The Euler method (fixed step-length)	29
	RK2(fixed step-length)	52
	RK4(fixed step-length)	105.353
[Min, max] time steps for ode solvers	ode23t	[1.022,196]
	ode23s	[3.2076,133]
	ode45	[0.5533,1.37]
	ode15s	[0.6381,150]
Steady water level in front of Grønvollfoss dam	For all solvers	17.0948 (m)

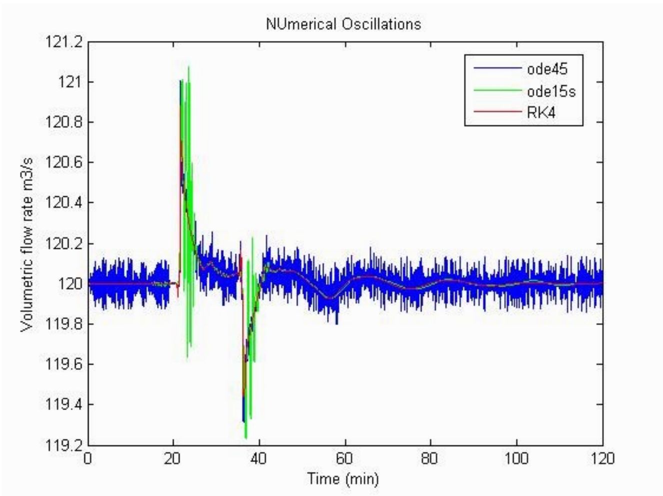

Figure 10. Numerical oscillation of group 02 solvers $\triangle t$ = 0.25 s.

spatial and time discretization is a good idea. Choice of $\triangle t$ necessarily has to be agreed with the CFL condition in order to achieve convergence with satisfactory accuracy in the final solution. For a selected $\triangle t$, which is higher than 0.7s, the Euler method produces oscillatory solution apart from the chosen $\triangle t$ satisfies the CFL condition. However, the RK2 and RK4 methods are quite stable while the Euler method shows oscillations. The numerical stability analysis indicated that the higher order variable step-length solvers are more oscillatory compared to higher order fixed step-length solvers. Final water height at Grønvollfoss dam is more or less similar with compared to different computations with variable step-length solvers and fixed step-length solvers. Results of the simulation study highly depend on the assumption made prior to simulation. The studied KP scheme has been found to be efficient and robust, and in a form suitable for use in control algorithm.

Acknowledgements

Kindly convey sincere thanks to the other project group members: Janitha Chandimal, Junyang Mao, and Obianuju Ezuka.

References

Fayssal Benkhaldoun, Saida Sari, and Mohammed Seaid. Projection finite volume method for shallow water flows. *Mathematics and Computers in Simulation*, 118:87 – 101, 2015. ISSN 0378-4754. doi:10.1016/j.matcom.2014.11.027.

Bernt Blindheim. A missing link? the case of norway and sweden: Does increased renewable energy production impact domestic greenhouse gas emissions? *Energy Policy*, 77:207 – 215, 2015. ISSN 0301-4215. doi:10.1016/j.enpol.2014.10.019.

Curtis F. Gerald and Patrick O. Wheatley. *Applied Numerical Analysis*. Pearson Education Inc., Boston, 2004.

Ian Gladwell, Larry Shampine, and S. Thompson. *Solving ODEs with MATLAB*. Cambridge University Press, New York, NY, USA, 2003. ISBN 0521530946.

Alexander Kurganov and Doron Levy. Central-upwind schemes for the Saint-Venant system. *Mathematical Modelling and Numerical Analysis*, 36(3): 397–425, 2002. doi:10.1051/m2an:2002019.

Alexander Kurganov and Eitan Tadmor. New high-resolution central schemes for nonlinear conservation laws and convection-diffusion equations. *Journal of Computational Physics*, 160(1):241 – 282, 2000. ISSN 0021-9991. doi:10.1006/jcph.2000.6459.

Randall J. LeVeque. *Numerical Methods for Conservation Laws*. Lectures in Mathematics, ETH Zurich. Birkhäuser Basel, 2nd edition, 1992. ISBN 978-3-0348-8629-1. doi:10.1007/978-3-0348-8629-1.

Xu-Dong Liu and Eitan Tadmor. Third order nonoscillatory central scheme for hyperbolic conservation laws. *Numerische Mathematik*, 79(3):397–425, May 1998. ISSN 0945-3245. doi:10.1007/s002110050345.

Haim Nessyahu and Eitan Tadmor. Non-oscillatory central differencing for hyperbolic conservation laws. *Journal of Computational Physics*, 87(2):408–463, April 1990. ISSN 0021-9991. doi:10.1016/0021-9991(90)90260-8.

Roshan Sharma. Second order scheme for open channel flow. Technical report, USN Open Archive, University College of Southeast Norway, 2015. URL `http://hdl.handle.net/11250/2438453`.

David J. Silvester, John W. Dold, and David Francis Griffiths. *Essential Partial Differential Equations: Analytical and Computational Aspects*. Springer International Publishing, 2015. ISBN 978-3-319-22569-2.

H. K. Versteeg and W. Malalasekera. *An introduction to computational fluid dynamics*. Pearson Education, Upper Saddle River, United States, 2nd edition, 2007. ISBN 9780131274983.

Liubomyr Vytvytskyi, Roshan Sharma, and Bernt Lie. Model based control for run-of-river system. Part 1: Model implementation and tuning. *Modeling, Identification and Control*, 36(4):237–249, 2015. doi:10.4173/mic.2015.4.4.